

*Communication*

## **Study of the Origin of Bending Induced by Bimetallic Effect on Microcantilever**

**Daniel Ramos, Johann Mertens, Montserrat Calleja and Javier Tamayo\***

BioNanoMechanics Lab, National Centre for Microelectronics, IMM-CNM, CSIC Isaac Newton 8 (PTM), Tres Cantos 28760, Madrid, Spain

\* Author to whom correspondence should be addressed. jtamayo@imm.cnm.csic.es

*Received: 30 July 2007 / Accepted: 4 September 2007 / Published: 5 September 2007*

---

**Abstract:** An analytical model for predicting the deflection and force of a bimaterial cantilever is presented. We introduce the clamping effect characterised by an axial load upon temperature changes. This new approach predicts a non linear thermal dependence of cantilever strain. A profilometry technique was used to measure the thermal strain. Comparison with experimental results is used to verify the model. The concordance of the analytical model presented with experimental measurements is better than 10%..

**Keywords:** cantilever, stress, strain, temperature, Stoney's equation, axial force, profile.

---

### **1. Introduction**

Atomic force microscope (AFM) cantilevers are known to be very sensitive to temperature [1]. Bimaterial microcantilevers have been used for a large number of applications that take advantage of this thermal sensitivity, as well as the reduction in the size of the probe and the high parallelizability, that improve the sensitivity and spatial resolution of the measurements [2]. These applications have included spatially-resolved calorimetry [3-7], ferromagnetic resonance [8], thermomechanical data storage [9-10], nanolithography [11-14] and thermal actuators [15-17].

It has been shown that silicon microcantilevers with a thin gold film on one side undergo measurable bending in response to temperature changes. This phenomenon is frequently referred to as the "bimetallic effect". In that particular case, the differential stress in the cantilever is created due to dissimilar thermal expansion coefficients of the silicon substrate and the gold coating. It has been estimated that the smallest heat change that can be detected using bimaterial microcantilevers lies in the femtojoule range [18].

Although previous publications [19, 20] in the field of micromechanics have described bimetallic cantilever microactuators, the derivation of the strain induced by temperature change for a cantilever clamped at one end is still incomplete. Furthermore, the origin of the force generated by such microactuators has been rarely discussed. In this communication, an analytical expression for the tip deflection and force of a bimetallic cantilever as a function of change in temperature is derived.

It will be demonstrated that the temperature dependent interfacial tension between gold and silicon layers leads to a non linear expression for the dependence of bending of the cantilever with temperature.

## 2. Theory

The Stoney's model describes the differential surface stress as a concentrated moment applied at the free end of the cantilever, Fig. 1a. Therefore, the governing equation of the beam deflection can be written as [21,22]

$$EI \frac{d^2 v(x)_{Stoney}}{dx^2} = M \quad (1)$$

where  $x$  is the spatial coordinate along the cantilever length,  $v(x)$  the vertical displacement,  $E$  is the Young's modulus,  $I$  the moment of inertia and  $M$  the applied moment. Taking into account the boundary conditions the solution of the above equation is a parabolic profile

$$v(x)_{Stoney} = \frac{Mx^2}{2EI} \quad (2)$$

For a rectangular beam, the moment of inertia is  $I = wt^3/12$  and the applied moment  $M = \sigma wt/2$ , where  $w$  and  $t$  are respectively the width and the thickness of the beam and  $\sigma$  the differential surface stress between the upper and lower sides. Therefore, for a prismatic cantilever the deflection curve is

$$v(x)_{Stoney} = \frac{3\sigma}{Et^2} x^2 \quad (3)$$

For a bilayer system, the Young modulus must be substituted by an effective value taking into account the thickness and the Young modulus of the both layers in the following way [24]

$$E_{eff} = \frac{E_f^2 \left(\frac{t_f}{t}\right)^4 + E_s^2 \left(\frac{t_s}{t}\right)^4 + 2E_f E_s \frac{t_f}{t} \frac{t_s}{t} \left(2\left(\frac{t_f}{t}\right)^2 + 2\left(\frac{t_s}{t}\right)^2 + 3\frac{t_f}{t} \frac{t_s}{t}\right)}{E_f \frac{t_f}{t} + E_s \frac{t_s}{t}} \quad (4)$$

where the subscripts  $f$  and  $s$  refer respectively the film and the substrate. For the case of  $t_f \ll t_s$ , the surface stress originated by the temperature change can be approximated as [25]

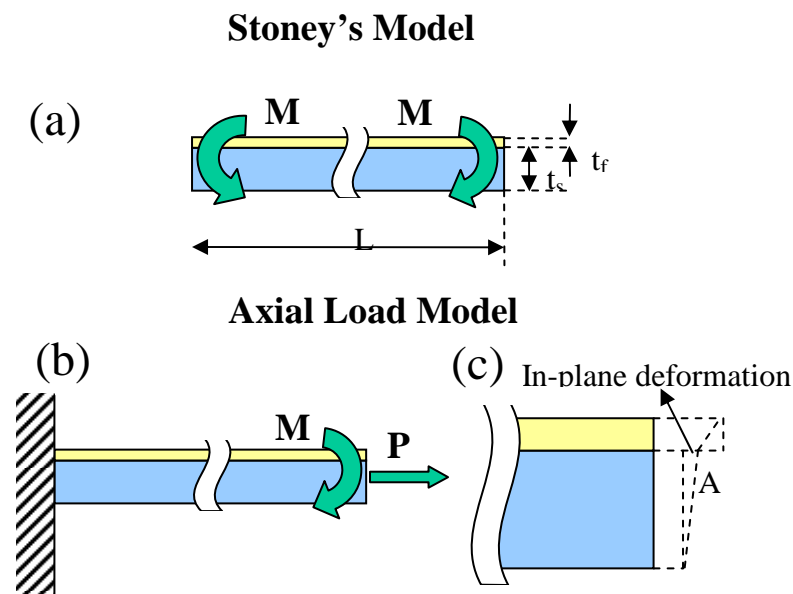
$$\sigma = E_f (\alpha_s - \alpha_f) \left( \frac{1 + \frac{E_f t_f^3}{E_s t_s^3}}{1 + \frac{t_f}{t_s}} \right) \Delta T \quad (5)$$

where  $\alpha_i$  are the thermal expansion coefficients of the film and the substrate and  $\Delta T$  is the external variation of temperature. Usually, the surface stress is deduced by measuring the tip displacement of the cantilever. Substituting eq. (5) in the deflection curve and fixing the free end at the coordinate  $x$  we obtain a linear dependence with the temperature

$$v(x=L)_{Stoney} = \frac{3L^2}{E_{eff} t^2} E_f (\alpha_s - \alpha_f) \left( \frac{1 + \frac{E_f t_f^3}{E_s t_s^3}}{1 + \frac{t_f}{t_s}} \right) \Delta T \quad (6)$$

where  $t=t_s+t_f$  is the total thickness. In this case the temperature dependence of the Young modulus of the cantilever materials has been neglected for the temperature variations commonly applied.

**Figure 1.** Scheme of (a) the Stoney's model for a plate deformation. The strain is derived from a moment applied at the free end of the cantilever. (b) the axial load model. An axial load component is added to take in account the effect of the clamping and also (c) the force induced by the displacement of the layer at the interface.



However, recent studies [25,26] have shown the necessity of including an axial load to complete the description of the dynamics of the cantilever deflection. This approach, depicted in Fig. 1b, leads to considering a different loading scenario and deformation system.

As it was discussed above, when the temperature changes, the difference in the thermal expansion coefficients and the Young's moduli of the cantilever materials leads to different linear deformations between the layers. Since the two materials are bonded, the interfacial line must reach some intermediate position, point A in Fig. 1c, causing an in-plane deformation. The physical origin of this deformation can be attributed to an axial load,  $P$ . Hence, the strain governing equation (1) must be changed to

$$EI \frac{d^4 v(x)_{Axial}}{dx^4} - P \frac{d^2 v(x)_{Axial}}{dx^2} = 0 \quad (7)$$

where the axial load depends on the system geometry  $P = w\sigma$ . Eq. 7 can be analytically solved,

$$v(x)_{Axial} = \frac{t}{2L \cosh\left(\frac{w\sigma(\Delta T)}{E_{eff} I} L\right)} \left[ \cosh\left(\frac{w\sigma(\Delta T)}{E_{eff} I} x\right) - 1 \right] \quad (8)$$

and at the cantilever free end the deflection can be written as

$$v(x=L)_{Axial} = \frac{t}{2L} \left[ 1 - \frac{1}{\cosh\left(\frac{w\sigma(\Delta T)}{E_{eff} I} L\right)} \right] \quad (9)$$

In this new loading scenario the temperature dependence of the deflection of the free end of the cantilever is not linear.

### 3. Experimental Section

We have used commercially available silicon cantilevers in our experiments (MikroMash). These cantilevers are rectangular; their nominal dimensions are 400  $\mu\text{m}$  in length, 100  $\mu\text{m}$  in width, and 1  $\mu\text{m}$  in thickness. Thermal evaporation at a pressure of  $10^{-5}$  Pa (0.2 nm/s) was then used to deposit a 2-nm-thick film of chromium and a 20 nm thick film of gold.

A cantilever holding cell was developed in which a medium vacuum can be reached in about 10 min by using a turbomolecular pump. Control valves are used to maintain a given gas pressure. A heating Peltier resistor mounted on the cell's outside wall can heat or cool the whole cell in a  $-223$  K/373 K range. The temperature within the cell can be controlled within 0.1% accuracy by using a model 325 Temperature Controller (Newport™). This T-control device ensures both thermistor operation by delivering output power of 17.5 W for the Peltier resistor and an ultra-stable temperature control ( $\pm 0.001^\circ\text{C}$ ) over a broad temperature range.

Cantilever bending is measured by home made scanning profilometry technique [27]. The readout technique combines the optical beam deflection method and the automated two-dimensional scanning of a single laser beam by means of voice-coil actuators. Fig. 2 shows a schematic drawing of the experimental device. A 3 mW laser diode is mounted onto a linear voice coil actuator that allow a nonhysteretic displacement over a range of several millimeters at speeds of up to 50 mm/s with an

accuracy of 100 nm. The laser beam is directed to illuminate the cantilever and a two-dimensional linear position detector (PSD) is arranged to collect the reflected beams. A convergent lens is used to reduce the spot size of the laser on the cantilevers to 5–10  $\mu\text{m}$ , approximately. The scanning is oriented parallel to the cantilever longitudinal axis in order to measure the cantilever profiles.

**Figure 2.** Sketch of the profilometry system. The laser is mounted in a 2-D voice-coil actuator. The beam can scan the cantilever array in the X and Y directions. The beam reflected of the cantilever surface is collected in a position sensitive diode.

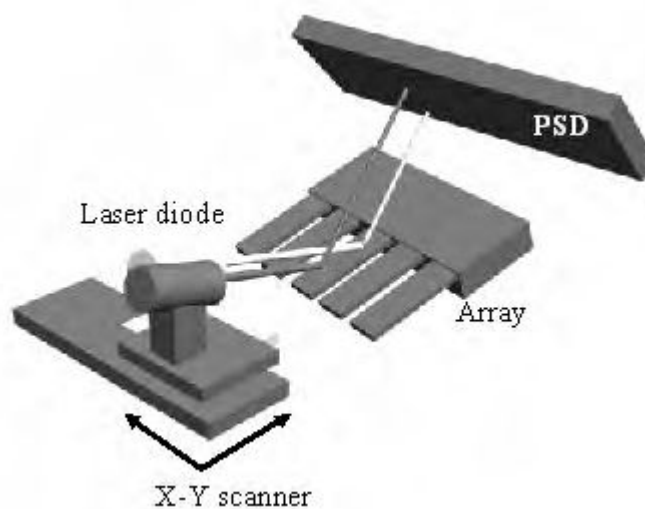
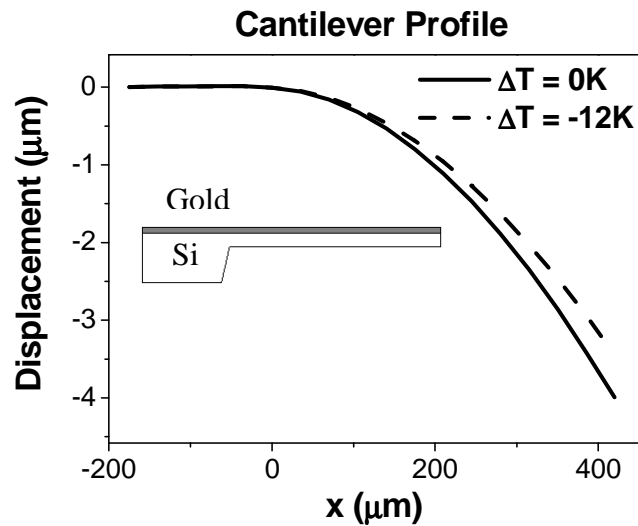


Fig. 3 shows the resulting cantilever profiles measured at  $P=10^{-2}$  Pa for two temperature variations  $\Delta T=0$  K and  $\Delta T=-12$  K. According to our T-control device,  $\Delta T=0$  K corresponds to a temperature of 298 K. The scan speed was set to 1 mm/s and the longitudinal axis of the cantilever was selected with a precision of 100 nm. The cantilever free ends were determined at the positions where the total light intensity collected by the PSD falls to the half. When increasing temperature, the cantilevers displace downward, towards the silicon side. The displacement arises from the compressive surface stress on the gold due to the differential expansion of gold and silicon layers.

The data obtained from this profilometry technique permit observing the cantilever shape and measuring the exact deformation induced by  $\Delta T$ . The end point deflection of the cantilever can also be measured. To elucidate the strain mechanisms of the cantilevers during temperature change, the initial cantilever profile ( $\Delta T=0$  K) was subtracted from the profiles at  $\Delta T=-12$  K. A maximum displacement of 53 nm is found at the free end of the cantilever. The measured deformation induced by the bimetallic effect was compared with the cantilever profile derived from the above models, as shown in Fig. 4a. As can be seen in this figure, for the same change of temperature, the Stoney's model predicts a cantilever displacement larger than the axial load model. This difference is a consequence of the flatten effect of the axial load. Therefore, for the same tip displacement, the surface stress derived from the Stoney's model is always smaller. The axial load model predict also a profile different in shape, as the force induced by the strain lead to a linear deformation component that differ from complete parabolic behavior expected from Stoney's model.

**Figure 3.** The cantilever profiles for  $\Delta T = 0\text{K}$  and  $\Delta T = -12\text{K}$  are presented. The cantilever bends upwards when the temperature decreases. A schematic depiction of the cantilever is also shown to relate the sign of the cantilever bending to the orientation of the bimetallic cantilever. The profiles were obtained in medium vacuum ( $10^{-2}\text{Pa}$ ).



**Fig. 4:** (a) Cantilever deformation predicted from the Stoney's model (dashed line) and the axial load model (solid line) for  $\Delta T = -12\text{K}$ . The two profiles are different in shape, as the axial load model does not show a complete parabolic behavior when temperature change. The experimental deflection profile fits with the axial load profile within a 10 % accuracy. (b) End tip deflection measured as function of  $\Delta T$ . Theoretical value calculated from the Stoney's model (dashed line) and the axial load model (solid line) are added for comparison. The parameters used in this fitting are:  $E_s = 169\text{ GPa}$ ,  $E_f = 79\text{ GPa}$ ,  $\alpha_s = 2.59 \cdot 10^{-6}\text{ K}^{-1}$ ,  $\alpha_f = 14.2 \cdot 10^{-6}\text{ K}^{-1}$ . The profiles were obtained in medium vacuum ( $10^{-2}\text{ Pa}$ ).

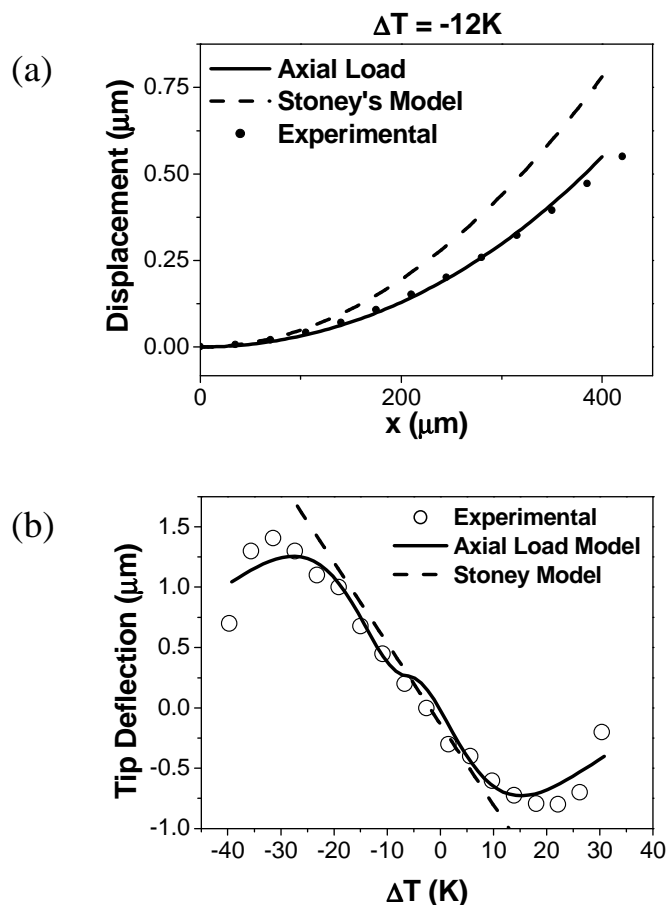


Fig. 4b shows the end tip deflection  $\delta$  measured as a function of temperature change  $\Delta T$  at  $P=10^{-2}$  Pa. The temperature  $T$  was gradually varied over a range between 235 K and 315 K. The bimetallic effect shows two different response regions as a function of  $\Delta T$ :

In the first region between  $\Delta T < -30\text{K}$  and  $\Delta T > 25\text{K}$ , the tip deflection increases with  $\Delta T$ , whereas it should decrease if we refer to the Stoney's model for a cantilever consisting of two layers with two different coefficients of thermal expansion. This behavior illustrates the difference between this classical model and the axial load model which fits well with the experimental data for  $\Delta T > 25\text{K}$ .

In the second region; for  $\Delta T > -30\text{K}$  and  $\Delta T < 25\text{K}$ ,  $\delta$  decreases following a linear dependence with  $\Delta T$  of 43 nm/K. The Stoney's model predict a larger slope of -67 nm/K. Hence, the Stoney's model prediction is also not accurate for small  $\Delta T$ .

The in-plane strain of the interface at the interface of gold and silicon layer film may explain the nonlinearity in the stress variation with  $\Delta T$ . The independent thermal strains of the two cantilever layers induce an axial force. The cantilever stops bending when the applied stress induced by the thermal change exceeds axial force coefficient. This force can be considered as bulk effects because the temperature change affects the whole of the thickness. This is the main difference compared with the adsorption induced strain, where the generated stress is confined to the surface.

## Conclusions

In this work the origin of the bending caused by bimetallic effect has been studied. The bimetallic effect is theoretically modelled taking into account the forces involved in the thermal expansion of the two layers. As was shown in the theory, this load is responsible of a non-linear dependence of the tip deflection of the cantilever with the temperature variation. This theoretical conclusion was experimentally validated. The result of this work can be generalized to other geometries to improve the temperature control of bimaterial cantilever based device.

## Acknowledgements

The authors acknowledge financial support from Ministerio de Educación y Ciencia (TEC2006-10316/MIC), CSIC and Comunidad de Madrid (200550M056). D. Ramos acknowledges the Comunidad de Madrid fellowship.

## References and Notes

1. Mertens, J.; Finot, E.; Thundat, T.; Fabre, A.; Nadal, M.-H.; Eyraud, V.; Bourillot, E. Effects of temperature and pressure on microcantilever resonance response. *Ultramicroscopy* **2003**, *97*, 119.
2. King, W.P.; Saxena, S.; Nelson, B.A. Nanoscale thermal analysis of an energetic material. *Nano Letters* **2006**, *6*, 2145.
3. Nonnenmacher, M.; Wickramasinghe, H. K. Scanning probe microscopy of thermal conductivity and subsurface properties. *Applied Physics Letters* **1992**, *61*, 168.
4. Abedinov, N.; Grabiec, P.; Gotszalk, T.; Ivanov, Tz.; Voigt, J.; Rangelow, I.W. Micromachined piezoresistive cantilever array with integrated resistive microheater for calorimetry and mass detection. *Journal of Vacuum Science and Technology A* **2001**, *19*, 2884.

5. Gotsmann, B.; Durig, U. Thermally activated nanowear modes of a polymer surface induced by a heated tip. *Langmuir*, **2004**, *20*, 1495.
6. Berger, R.; Lang, H.; Gerber, C.; Gimzewski, J.; Fabian, J.; Scandella, L.; Meyer, E.; Guntherodt, H. Micromechanical thermogravimetry. *Chemical Physics Letter* **1998**, *294*, 363.
7. Pinnaduwege, L. A.; Wig, A.; Hedden, D. L.; Gehl, A.; Yi, D.; Thundat, T.; Lareau, R. T. Detection of trinitrotoluene via deflagration on a microcantilever. *Journal of Applied Physics* **2004**, *95*, 5871.
8. Wallis, T.M.; Moreland, J.; Riddle, B.; Kabos, P. Microwave power imaging with ferromagnetic calorimeter probes on bimaterial cantilevers. *Journal of Magnetism and Magnetic Material* **2005**, *286*, 320.
9. King, W. P.; Kenny, T. W.; Goodson, K. E.; Cross, G.; Despont, M.; Durig, U.; Rothuizen, H.; Binnig, G. K.; Vettiger, P. Atomic force microscope cantilevers for combined thermomechanical data writing and reading. *Applied Physics Letters* **2001**, *78*, 1300.
10. Mamin, H. J.; Fan, L. S.; Rugar, D.; Hoen, S. Tip-based data storage using micromechanical cantilevers. *Sensors and Actuators A: Physical* **1995**, *48*, 215-219.
11. Wang, D. A.; Bullen, J.; Zou, C.; Liu, J.; Mirkin, C. Thermally actuated probe array for parallel dip-pen nanolithography. *Journal of Vacuum Science and Technology B* **2004**, *22*, 2563.
12. Gotsmann, B.; Durig, U.; Frommer, J.; Hawker, C. J. Exploiting chemical switching in a Diels-Alder polymer for nanoscale probe lithography and data storage. *Advanced Functional Materials* **2006**, *16*, 1499.
13. Sheehan, P. E.; Whitman, L. J.; King, W. P.; Nelson, W. P. Nanoscale deposition of solid inks via thermal dip pen nanolithography. *Applied Physics Letter* **2004**, *85*, 1589.
14. Nishimura, S.; Takemura, Y.; Shirakashi, J. SPM local oxidation nanolithography with active control of cantilever dynamics. *Journal of Physics: Conference Series* **2007**, *61*, 1066.
15. Lalinský, T.; Burian, E.; Držík, M.; Hascík, S.; Mozolová, Z.; Kuzmík, J. Thermal actuation of a GaAs cantilever beam. *Journal of Micromechanics and Microengineering* **2000**, *10*, 293.
16. Grigorov, A.V.; Davis, Z.J.; Rasmussen, P.; Boisen A. A longitudinal thermal actuation principle for mass detection using a resonant micro-cantilever in a fluid medium. *Microelectronic Engineering* **2004**, *73*, 881.
17. Sulchek, T.; Minne, S. C.; Adams, J. D.; Fletcher, D. A.; Atalar, A.; Quate, C. F.; Adderton, D. M. Dual integrated actuators for extended range high speed atomic force microscopy. *Applied Physics Letters* **1999**, *75*, 1637.
18. Barnes, J.R.; Stephenson, R.J.; Welland, M.E.; Gerber, C.; Gimzewski, J.K. Photothermal spectroscopy with femtojoule sensitivity using a micromechanical device. *Nature* **1994**, *372*, 79.
19. Chu, W.-H.; Mehregany, M.; Mullen, R. L. Analysis of tip deflection and cantilever force of a bimetallic cantilever microactuator. *J. Micromech. Microeng.* **1993**, *3*, 4-7
20. Shuir, E. Stresses in bi-metal thermostats. *J. Appl. Mech.* **1986**, *53*, 657-660.
21. Stoney, G. G. The Tension of metallic films deposited by electrolysis. *Proc. R. Soc. London, Ser. A* **1909**, *82*, 172-175.
22. Timoshenko, S. Analysis of bi-metal thermostats. *J. Opt. Soc. Am.* **1925**, *11*, 233-255.

23. Yi, J. W.; Shih, W. Y.; Shih, W.-H. Effect of length, width, and mode on the mass detection sensitivity of piezoelectric unimorph cantilevers. *J. Appl. Phys.* **2002**, *91*, 1680-1686.
24. Hsueh, C. H. Modeling of elastic deformation of multilayers due to residual stresses and external bending. *J. Appl. Phys.* **2002**, *91*, 9652-9656.
25. MacFarland, A. W.; Poggi, M. A.; Doyle, M. J.; Bottomley, L. A.; Colton, J. S. Influence of surface stress on the resonance behavior of microcantilevers. *Appl. Phys. Letts.* **2005**, *87*, 053505.
26. Zhang, Y.; Zhao, Y.-P. Applicability range of Stoney's formula and modified formulas for a film/substrate bilayer. *J. Appl. Phys.* **2006**, *99*, 053513.
27. Mertens, J.; Álvarez, M.; Tamayo, J. Real-time profile of microcantilevers for sensing applications. *Appl. Phys. Lett.* **2005**, *87*, 2344102.